

# Reversible Transformations of Gold Nanoparticle Morphology

Savka I. Stoeva,<sup>†,||</sup> Vladimir Zaikovski,<sup>§</sup> B. L. V. Prasad,<sup>†,⊥</sup> Peter K. Stoimenov,<sup>†,#</sup>  
Christopher M. Sorensen,<sup>‡</sup> and Kenneth J. Klabunde\*,<sup>†</sup>

*Departments of Chemistry and Physics, Kansas State University, Manhattan, Kansas 66506,  
and Boreskov Institute of Catalysis, Novosibirsk 630090, Russia*

*Received June 24, 2005. In Final Form: September 1, 2005*

Herein is reported a metamorphosis taking place in a gold nanosized system. The observed phenomenon of shape and size transformations was found to be completely reversible. Unlike most procedures in the literature where shape and size control occur in the synthetic step by adding growth- and shape-controlling agents such as surfactants or polymers, in this system postsynthetic changes in shape and size can be carried out simply by changing the ratio of reactive, competing reagents, more specifically, alkylthiols versus tetralkylammonium salts. Interestingly, the transfer of gold metal occurs (large prismatic particles to small particles and vice versa) under the influence of reagents that do not cause such interactions with bulk gold. All intermediate steps of the morphology change were observed using HRTEM and electron diffraction. The processes of breaking down and “welding back” solid metal nanoparticles occur under mild conditions and are remarkable examples of the unique chemical properties of nanomaterials. The described process is expected to be relevant to other nanoscale systems where similar structural circumstances could occur.

## Introduction

Nanoscale materials, as an intermediate state between molecular and bulk matter, possess unique chemical and physical properties that drive significant fundamental and technological interest. Materials characteristics drastically change as the size of the constituting particles approaches the nanoscale regime. The change in properties is a result of the presence of a small number of atoms in each particle and a large surface-to-volume ratio due to the large fraction of atoms that reside on the particle surface. Size and shape are the two major factors that determine nanoparticle properties. High-quality nanoparticles from different materials can be routinely synthesized with different sizes and functional groups,<sup>1</sup> and methods for the large-scale production of some metal and semiconductor particles have been developed.<sup>2</sup> Nanostructures with diverse shapes have been synthesized such as cubes,<sup>3</sup> prisms,<sup>4</sup> rods,<sup>5</sup> stars,<sup>6</sup> tetrapods,<sup>7</sup> hollow spheres,<sup>8</sup> and hollow cubes.<sup>3b</sup> The general strategy to

promote anisotropic crystal growth is to induce different relative growth rates of crystallographic faces.<sup>9</sup> Anisotropic growth of nanoparticles in solution is usually achieved by the presence of molecules in the system that have a preferential binding to different crystallographic faces while the particles nucleate and grow in solution. Different nanoparticle shapes have been achieved so far, but a complete understanding of the factors determining the particle morphology has not been attained.

Here we describe a unique protocol for reversibly manipulating the size and morphology of gold nanoparticles after the particles are already prepared. This phenomenon is induced by specific types of molecules interacting with the gold nanoparticles: (1) molecules (ligands) that have functional groups with a strong affinity for adsorption on gold surfaces with the formation of relatively strong bonds, such as alkanethiols (RSH),<sup>10,11</sup> and (2) positively charged quaternary alkylammonium surfactants such as didodecyltrimethylammonium bromide (DDAB). The morphology and dimensions of the gold nanoparticles are reversibly controlled in solvent at room temperature or reflux depending upon the relative ratio of alkanethiol to DDAB. The results presented here provide direct insight into the changes in nanoparticle morphology that occur at intermediate steps during the action of different stabilizing molecules.

\* Corresponding author. E-mail: kenjk@ksu.edu. Phone: 785-532-6849. Fax: 785-532-6666.

<sup>†</sup> Department of Chemistry, Kansas State University.

<sup>§</sup> Department of Physics, Kansas State University.

<sup>||</sup> Boreskov Institute of Catalysis.

<sup>⊥</sup> Present address: Northwestern University, Department of Chemistry, Evanston, Illinois 60208-3113.

<sup>‡</sup> Present address: Materials Chemistry Division, National Chemical Laboratory, Pune 411 008, India.

<sup>#</sup> Present address: UC Santa Barbara, Department of Chemistry, Santa Barbara, California 93106.

(1) (a) Cushing, B. L.; Kolesnichenko, V. L.; O'Connor, C. J. *Chem. Rev.* **2004**, *104*, 3893–3946. (b) Murray, C. B.; Kagan, C. R.; Bawendi, M. G. *Annu. Rev. Mater. Sci.* **2000**, *30*, 545–610.

(2) (a) Stoeva, S.; Klabunde, K. J.; Sorensen, C. M.; Dragieva, I. J. *Am. Chem. Soc.* **2002**, *124*, 2305–2311. (b) Jana, N. R.; Peng, X. J. *Am. Chem. Soc.* **2003**, *125*, 14280–14281. (c) Li, J. J.; Wang, Y. A.; Guo, W.; Keay, J. C.; Mishima, T. D.; Johnson, M. B.; Peng, X. J. *Am. Chem. Soc.* **2003**, *125*, 12567–12575.

(3) (a) Ahmadi, T. S.; Wang, Z. L.; Green, T. C.; Henglein, A.; El-Sayed, M. A. *Science* **1996**, *272*, 1924–1925. (b) Sun, Y.; Xia, Y. *Science* **2002**, *298*, 2176–2179.

(4) (a) Jin, R.; Cao, Y.; Mirkin, C. A.; Kelley, K. L.; Schatz, G. C.; Zheng, J. G. *Science* **2001**, *294*, 1901–1903. (b) Jin, R.; Cao, Y.; Hao, E.; Metraux, G. S.; Schatz, G. C.; Mirkin, C. A. *Nature* **2003**, *425*, 487–490.

(5) (a) Peng, X.; Manna, L.; Yang, L.; Wickham, J.; Scher, E.; Kadavanich, A.; Alivisatos, A. P. *Nature* **2000**, *404*, 59–61. (b) Busbee, B. D.; Obare, S. O.; Murphy, C. J. *Adv. Mater.* **2003**, *15*, 414–416.

(6) Lee, S.; Jun, Y.; Cho, S.; Cheon, J. *J. Am. Chem. Soc.* **2002**, *124*, 11244–11245.

(7) (a) Milliron, D. J.; Hughes, S. M.; Cui, Y.; Manna, L.; Li, J.; Wang, L.; Alivisatos, A. P. *Nature* **2004**, *430*, 190–195. (b) Chen, S.; Wang, Z. L.; Ballato, J.; Foulger, S. H.; Carroll, D. L. *J. Am. Chem. Soc.* **2003**, *125*, 16186–16187.

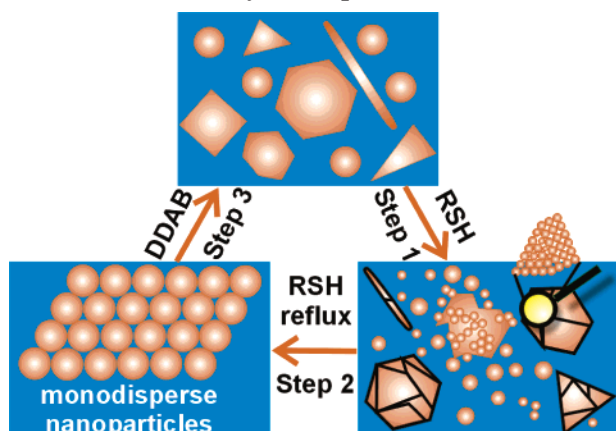
(8) Yin, Y.; Rioux, R. M.; Erdonmez, C. K.; Hughes, S.; Somorjai, G. A.; Alivisatos, A. P. *Science* **2004**, *304*, 711–714.

(9) (a) Puentes, V. F.; Krishnan, K. M.; Alivisatos, A. P. *Science* **2001**, *291*, 2115–2117. (b) Murphy, C. J. *Science* **2002**, *298*, 2139–2141. (c) Pileni, M. P. *Nat. Mater.* **2003**, *2*, 145–150.

(10) Bain, C. D.; Evall, J.; Whitesides, G. M. *J. Am. Chem. Soc.* **2003**, *111*, 7164–7175.

(11) Different chain length alkanethiols (C4–C18) were found to act in the same way.

**Scheme 1. Reversible Change of Larger Polyhedral Nanoparticles into Smaller, Monodisperse Ligand-Stabilized Spherical Particles that Order into Nanocrystal Superlattices**



### Materials and Methods

**Gold Nanoparticle Synthesis.** Starting polyhedral-shaped gold nanoparticles were synthesized by sodium borohydride reduction of  $\text{AuCl}_3$  dissolved in toluene in the presence of DDAB. In a typical reaction, 0.034 g of  $\text{AuCl}_3$  (99.99%, Aldrich) was dissolved by sonication (20 min, Branson sonicator) in a solution of 0.104 g of DDAB (0.02 M final concentration, Fluka) in 10 mL of toluene (freshly degassed) under an argon atmosphere, resulting in a dark orange-red solution.<sup>12</sup> Reduction of the gold salt was carried out by the dropwise addition of 30  $\mu\text{L}$  of freshly prepared 9.3 M  $\text{NaBH}_4$  (Aldrich) aqueous solution. The reaction mixture was magnetically stirred for 15 min to ensure the completion of the process. Dark purple Au colloid formed at the end of the process.

**Digestive Ripening.** Dodecanethiol (Aldrich) was added to the primary gold colloid in an  $n(\text{RSH})/n(\text{Au}) = 30:1$  molar ratio, followed by anhydrous ethanol (Aldrich) precipitation to remove reaction byproducts. The supernatant was decanted, and the gold particle–thiol precipitate was vacuum dried and then redispersed in the corresponding amount of toluene and alkanethiol. Reflux of the mixture (90 min) under an argon atmosphere led to the formation of monodisperse  $\sim 5$  nm Au particles.

**Reverse Digestive Ripening.** After reflux, the excess alkanethiol was removed from the system by ethanol precipitation, supernatant removal, and redispersion in toluene. DDAB was added to the system, keeping the molar ratio  $n(\text{DDAB})/n(\text{Au}) = 2:1$ .

**Structural Analysis.** Samples for TEM were prepared by placing a 3  $\mu\text{L}$  drop of the colloidal solution onto a carbon-coated Formvar copper grid. The grids were allowed to dry in a dust-free area for several hours. High-resolution TEM (HRTEM) imaging was done with a JEM-2010 (JEOL, Japan) with 1.4 Å lattice resolution and 200 kV accelerating voltage. Selected-area electron diffraction (SAED), computer-simulated fast Fourier transformed (FFT) images, and Fourier filtration (IFFT) were used for the in-depth structural analysis of the particles.

### Results and Discussion

Scheme 1 illustrates three major steps in the reversible process of nanoparticle morphology transformation observed in this study. Step 1 is the breaking up of large polyhedral particles to form small spherical particles, which is induced by alkanethiols at room temperature. Step 2 represents a complete transformation of a polydisperse colloid into a nearly monodisperse one by refluxing the system (digestive ripening) in toluene solvent

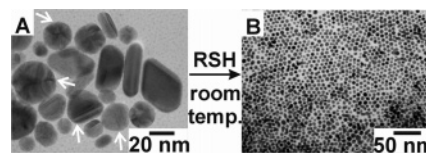


**Figure 1.** Ligand-induced break up of (A) large polyhedral gold particles at ambient conditions into (B) small spherical particles. Lattice distortions (designated by arrows) in the particles in A lead to the appearance of areas with different contrast in the TEM images (Moiré patterns).

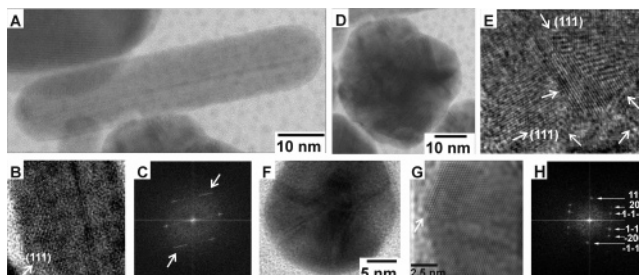


**Figure 2.** TEM and electron diffraction images of representative polyhedral gold particles from the colloid in Figure 1A. (A) HRTEM of a rodlike nanoparticle with defects in the atomic arrangement parallel to the (111) lattice planes and the corresponding Fourier-filtered image (B) of a part of the particle and the FFT image (C) showing elongation of the diffraction reflexes. (D) HRTEM of an MTP particle with nonparallel (111) twinning boundaries designated by arrows in the corresponding Fourier-filtered image in E. (F) HRTEM of a decahedral particle. One of the twinning boundaries is clearly seen on the Fourier-filtered image in G. Twinning results in the splitting of the diffraction reflexes in the FFT image in H.

with excess alkanethiol, yielding nanoparticles that are highly uniform in size and shape and thus have a strong propensity to self-assemble into long-range-ordered nanocrystal superlattices.<sup>2a,13</sup> Step 3 (reverse of steps 1 and 2) shows the transformation of spherical particles back into larger polyhedral particles by the action of excess DDAB.

The primary large polyhedral gold particles were synthesized by an inverse micelle procedure by the reduction of  $\text{AuCl}_3$  in a DDAB/toluene solution with aqueous  $\text{NaBH}_4$  as described previously.<sup>13b</sup> Alkanethiol (the results presented here include dodecanethiol) or DDAB was added to the colloid at different stages of Scheme 1, keeping the molar ratios of  $n(\text{DDAB})/n(\text{Au}) = 2:1$  and  $n(\text{RSH})/n(\text{Au}) = 30:1$ . Before each step, the gold colloid was separated from excess RSH or DDAB by ethanol precipitation, supernatant removal, vacuum drying, and redispersion in toluene. The size and shape of the particles at the different stages were studied by transmission electron microscopy (TEM).

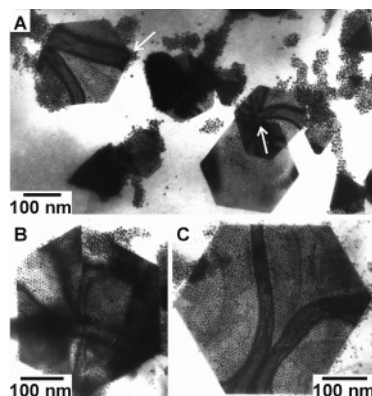
Figure 1 illustrates the complete break up of large (10–100 nm) polyhedral particles to small (2–10 nm) spherical particles by RSH addition at ambient conditions. We believe that the reason for this facile break up is the highly defective structure of the polyhedral particles. Defects such as twinning boundaries and stacking faults are abundant in these particles.

Figure 2A shows a HRTEM image of a rodlike particle that possesses many defects in the arrangement of the gold atoms. The defects are parallel to the (111) lattice planes and are visible from the Fourier-filtered image in Figure 2B and confirmed by the elongation of the diffraction spots in the FFT image in Figure 2C (designated

(12) The concentration of the DDAB solution is above the cmc in toluene ( $\sim 10^{-3}$  M from Seoud, E. In *Reversed Micelles and Water-in-Oil Microemulsions in Organized Assemblies in Chemical Analysis*; Hinze, W. L., Ed.; Wiley: New York, 1994; pp 1–37.

(13) (a) Lin, X. M.; Sorensen, C. M.; Klabunde, K. J. *J. Nanopart. Res.* **2000**, 2, 157–164. (b) Stoeva, S. I.; Prasad, B. L. V.; Uma, S.; Stoimenov, P. K.; Zaikovski, V.; Sorensen, C. M.; Klabunde, K. J. *J. Phys. Chem. B* **2003**, 107, 7441–7448.





**Figure 3.** (A) TEM micrograph illustrating the breaking-up process of large polyhedral particles to small spherical ones upon RSH addition at ambient conditions. (B and C) Magnified TEM images showing the breaking-up process. Note the defects in the polyhedral particles and the small spherical particles streaming out.

by arrows). Figure 2D illustrates a typical multiply twinned particle (MTP) present in the primary gold colloids. MTPs are often formed by gold and other face-centered cubic (fcc) metals.<sup>14</sup> The particle presented in Figure 2D contains nonparallel (111) twinning boundaries clearly visible from Figure 2E (designated by arrows). Another representative MTP gold nanoparticle is shown in the HRTEM micrograph in Figure 2F. The corresponding FFT image in Figure 2H shows the split reflections in the diffraction pattern resulting from the twinning. The atomic-resolution Fourier-filtered image in Figure 2G illustrates one of the twinning boundaries present in the particle in Figure 2F. The presence of twinning boundaries, especially in particles larger than  $\sim 10$  nm, leads to the appearance of strong microstresses in their structure, a decrease in the lattice stabilization energy, and higher chemical reactivity.<sup>13</sup>

These considerations may help explain why bulk gold is not attacked by alkanethiols, whereas these defective polyhedral nanoparticles are. Apparently, the crystal interfaces in these polyhedral nanoparticles cause great strain and can serve as attack sites. The above suggestion is supported by the TEM micrographs presented in Figure 3A–C that were obtained on a sample at an intermediate stage. Small spherical particles are observed near the original highly defective particles (Figure 3). Such areas were often found (especially in the case of decanethiol addition) in the TEM samples of gold colloids imaged immediately after RSH addition to the polyhedral particles. Besides the remnants of the larger particles (Figure 3), thin, less-defective crystals were occasionally found in the samples immediately after RSH addition, which suggests that the attacking alkylthiol molecules caused a thinning of the larger starting polyhedrons. Eventually, all of the polyhedral particles were converted to small ( $<10$  nm) spherical particles.

Initially, these small, spherical particles are not monodisperse, but upon reflux (digestive ripening), monodisperse nanocrystals with an average diameter of 4.6 nm form that are the stable products under the given conditions.<sup>12,15</sup> However, a remarkable finding is that this

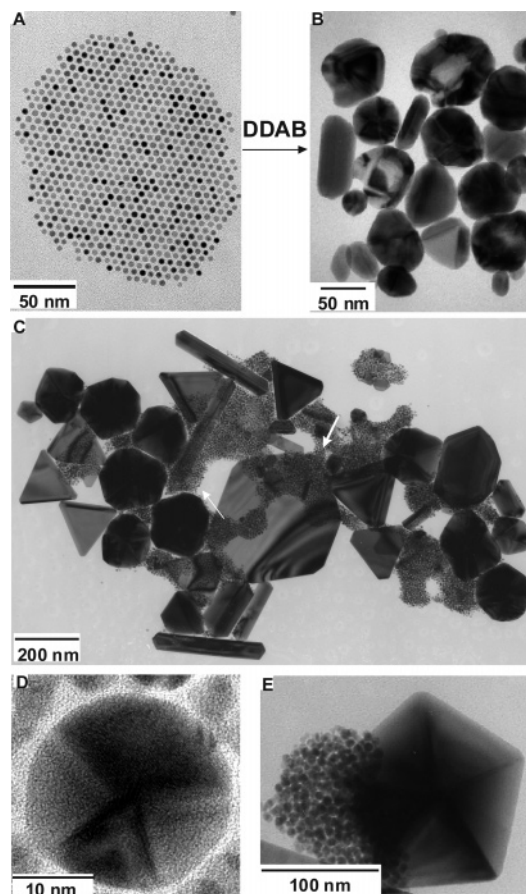


**Figure 4.** (A) Uniform particles formed after solvent reflux of the primary gold colloid in excess RSH. (B) Defective polyhedral particles formed after treatment of A with excess DDAB at ambient conditions or reflux. (C) Representative multiply twinned particles present in the colloids after DDAB treatment. Arrows show regions where parts of the particles are composed of closely spaced small spherical particles. (D) Representative decahedral particle present in the system after DDAB addition to A. (E) Magnified particle with partially rebuilt structure.

ligand attachment/digestive ripening can be reversed by the removal of excess attacking ligand (alkanethiol) and the addition of an excess of an ionic surfactant (DDAB) either at room temperature or at toluene reflux. Figure 4A shows the digestively ripened, monodisperse  $(\text{Au})_n$ -thiol particles, which convert to larger, variously shaped particles shown in Figure 4B. Indeed, the structures shown in Figure 4B are very similar to those originally formed by the gold salt reduction step for nanoparticle synthesis in the presence of DDAB (Figure 1A). Figure 4C is another image of these reformed polyhedral particles with some remaining small particles that have not yet been converted back. Another similar image closer up is shown in Figure 4E. Figure 4D illustrates a multiply twinned decahedral particle with 5-fold pentagonal symmetry. Interestingly, some of the particles are partially rebuilt like the particle in Figure 4E with the rest of the particle composed of closely arranged spherical particles. The arrows in Figure 4C designate other partially rebuilt particles. These results confirm that the large polyhedral particles are rebuilt from the small spherical ones upon DDAB addition.

How does this unprecedented, low-temperature metal particle growth take place? The DDAB must perform at least two functions: it must disrupt the thiol–metal ligand bonding and help guide the regrowth of larger particles, which is really a “welding” of smaller spherical particles together. Indeed, the presence of DDAB or the similar

(14) (a) Wang, Z. L. *J. Phys. Chem. B* **2000**, *104*, 1153–1175. (b) Marks, L. D. *Rep. Prog. Phys.* **1994**, *57*, 603–649. (c) Klabunde, K. J., Mulukutla, R. S. In *Nanoscale Materials in Chemistry*; Klabunde, K. J., Ed.; Wiley-Interscience: New York, 2001; pp 223–261.

(15) (a) Prasad, B. L. V.; Stoeva, S. I.; Sorensen, C. M.; Klabunde, K. J. *Langmuir* **2002**, *18*, 7515–7520. (b) Prasad, B. L. V.; Stoeva, S. I.; Sorensen, C. M.; Klabunde, K. J. *Chem. Mater.* **2003**, *15*, 935–942.

cetyltrimethylammonium bromide has promoted unexpected behavior in other systems, such as the growth of metal tips onto semiconductor quantum rods,<sup>16</sup> the reshaping of metal nanoshells,<sup>17</sup> and the growth of gold and iron nanorods.<sup>5b,18</sup> These phenomena are not fully understood, nor is the behavior of DDAB under the current circumstances (Figure 4) understood. However, it cannot be coincidental that the effect of adding an ionic reagent that dissolves in the solvent at hand causes a destabilization of the colloid and flocculation/precipitation of larger particles, as is always the case with aqueous systems where particle repulsion (colloid stabilization) is disrupted by the added ionic reagent.<sup>19</sup> Such charging effects in an organic media of much lower dielectric constant must be quite small in comparison to those in aqueous systems. However, our results suggest that the DDAB does disrupt any such charged particle repulsion effects as well as help carry away thiol ligands, and gold–gold metal bonding is

facilitated. Interestingly, if the excess DDAB is removed from the larger polyhedral particles and an excess of thiol is again added, then the system returns, upon toluene reflux, to uniform 5 nm thiol-stabilized spherical particles as shown in Figure 4A. Thus, the monodisperse spherical particle to polyhedral larger particle transformation is completely reversible and is dependent on the variance of relative concentration of either the alkylthiol or DDAB surfactant.

In summary, the size and shape of gold nanoparticles can be manipulated by added reagents that serve to carry out “chemical machining,” and these processes are reversible. These results demonstrate the high reactivity of metal nanoparticles even under mild conditions and suggest that other nanomaterials could be similarly manipulated and should be dependent only on the proper choice of chemical machining reagents.

(16) Mokari, T.; Rothenberg, E.; Popov, I.; Costi, R.; Banin, U. *Science* **2004**, *304*, 1787–1790.

(17) Aguirre, C. M.; Kaspar, T. R.; Radloff, C.; Halas, N. J. *Nano Lett.* **2003**, *3*, 1707–1711.

(18) Park, S.; Kim, S.; Lee, S.; Khim, Z. G.; Char, K.; Hyeon, T. *J. Am. Chem. Soc.* **2000**, *122*, 8581–8582.

(19) Brinker, C. J.; Scherer, G. W. In *Sol–Gel Science*; Academic Press: San Diego, 1990; p 242.

**Acknowledgment.** We acknowledge the partial support of the National Science Foundation, the National Aeronautics and Space Administration, and the BioServe Institute at Kansas State University.

LA051699V